Melanin-concentrating hormone is a critical mediator of the leptin-deficient phenotype

Gabriella Segal-Lieberman*[†][‡], Richard L. Bradley*[†], Efi Kokkotou*[†], Michael Carlson*, Daniel J. Trombly*, Xiaomei Wang*, Sarah Bates*[†], Martin G. Myers, Jr.*[†][§], Jeffrey S. Flier*[†][§], and Eleftheria Maratos-Flier*[†][¶]

*Research Division, Joslin Diabetes Center, Boston, MA 02215; [§]Division of Endocrinology, Beth Israel Deaconess Medical Center, Boston, MA 02215; and [†]Department of Medicine, Harvard Medical School, Boston, MA 02215

Energy homeostasis is regulated by a complex network involving peripheral and central signals that determine food intake and energy expenditure. Melanin-concentrating hormone (MCH) plays an essential role in this process. Animals treated with MCH develop hyperphagia and obesity. Ablation of the prepro-MCH gene leads to a lean phenotype, as does ablation of the rodent MCH receptor, MCHR-1. MCH is overexpressed in the leptin-deficient *ob/ob* mouse, and we hypothesized that ablation of MCH in this animal would lead to attenuation of its obese phenotype. Compared with *ob/ob* animals, mice lacking both leptin and MCH (double null) had a dramatic reduction in body fat. Surprisingly, the hyperphagia of the *ob/ob* mouse was unaffected. Instead, leanness was secondary to a marked increase in energy expenditure resulting from both increased resting energy expenditure and locomotor activity. Furthermore, double-null mice showed improvements in other parameters impaired in *ob/ob* mice. Compared with *ob/ob* mice, double-null animals had increased basal body temperature, improved response to cold exposure, lower plasma glucocorticoid levels, improved glucose tolerance, and reduced expression of stearoyl-CoA desaturase 1 (SCD-1). These results highlight the importance of MCH in integration of energy homeostasis downstream of leptin and, in particular, the role of MCH in regulation of energy expenditure.

Melanin-concentrating hormone (MCH), a 19-aa neuropeptide, is the product of the prepro-MCH gene and is expressed exclusively within the lateral hypothalamus. MCH neurons make monosynaptic projections throughout the neuraxis including the cortex and hindbrain, suggesting that MCH regulates complex motivated behaviors (1). A role for MCH in energy homeostasis emerged from studies demonstrating differential MCH gene expression in leptin-deficient *ob/ob* mice, where MCH mRNA was overexpressed 2- to 3-fold compared with normal-weight littermates, in both fed and fasted states (2). Furthermore, MCH administration into the lateral ventricle of rats caused an acute and rapid increase in feeding (2, 4). Genetic evidence for a role of MCH in energy balance was derived from a model of MCH gene ablation, which produced a lean phenotype associated with a decrease in feeding and an increase in resting energy expenditure (3), and also from a model of transgene-derived eutopic overexpression, which produced mild obesity (5). Recently, chronic infusions of MCH were shown to produce hyperphagia and obesity in mice (6) and rats (7).

Based on the foregoing evidence, we hypothesized that MCH contributed to the hyperphagia seen in *ob/ob* mice (8) and predicted that mice lacking both MCH and leptin would show an attenuated obesity phenotype secondary to decreased feeding. Therefore, we performed a series of crosses of MCH^{−/−} mice and *ob/+* mice to generate mice lacking both leptin and MCH, i.e., MCH^{−/−} *ob/ob* mice, designated double null.

Double-null mice had marked attenuation of obesity and associated metabolic and endocrine abnormalities of leptin deficiency. Remarkably, food intake was no different in *ob/ob* mice vs. double-null animals, and the improvement in obesity resulted exclusively from an increase in energy expenditure, with double-

null mice having an increased resting metabolic rate, a significant increase in locomotor activity, and an improved ability to thermoregulate in response to environmental cold exposure. These results indicate that MCH is a key neuropeptide acting downstream of leptin and that MCH is required for manifestation of the full *ob/ob* phenotype. In particular, MCH is an essential mediator of the central neural circuit by which leptin deficiency suppresses energy expenditure through effects on both resting metabolic rate and locomotor activity.

Materials and Methods

Animals. All studies were approved by the Joslin Diabetes Center Animal Care and Use Committee. Male mice were weaned at 3–4 weeks of age, genotyped, and housed, two to four mice per cage, with access to 9% fat food (Purina Formulab 5008) and water ad libitum at 24°C under an alternating 12-h light/dark cycle.

Generation of MCH^{−/−} *ob/ob* Mice. Mice deficient in both MCH and leptin were obtained by breeding MCH^{−/−} (3), backcrossed for six generations onto a C57BL/6 background at Taconic Farms, to C57BL/6 *ob/+* mice (The Jackson Laboratory). To generate *ob/ob* mice lacking the MCH gene, MCH^{−/−} males were first bred to *ob/+* females to create compound heterozygotes (MCH^{+/−} *ob/+*). In a second cross, compound heterozygotes were bred with each other, and MCH^{−/−} *ob/+* as well as MCH^{+/+} *ob/+* offspring were identified. In a third set of crosses, MCH^{−/−} *ob/+* mice were bred to each other to produce MCH^{−/−} *ob/ob* animals and MCH^{−/−} OB/OB animals. In parallel, MCH^{+/+} *ob/+* mice were bred to each other to produce MCH^{+/+} *ob/ob* as well as MCH^{+/+} OB/OB (WT) mice.

Genotyping. Genotypes were confirmed by PCR amplification of genomic DNA. In MCH^{−/−} mice, primers targeting the PGK-neo cassette (3) were used for the PCR. The primers were: for MCH, 5′-GAATTTGGAAGATGACATAGTAT-3′ (sense) and 5′-CAGCCCGGTGAGTTACAAGATTCT-3′ (antisense); for PGK-neo, 5′-CGGGTAGGGGAGGCGCT-3′ (sense) and 5′-GCGCAAGGAACGCCCGTCGTG-3′ (antisense); for the OB gene, 5′-GCCAATGACCTGGAGAATCTC-3′ (sense) and 5′-AGGACGCCATCCAGGCTCTC-3′ (antisense); and for the *ob* mutation, 5′-GCCAATGACCTGGAGAATCTCT-3′ (sense) and 5′-AGGACGCCATCCAGGCTCTC-3′ (antisense).

Glucose Tolerance Tests. Mice were fasted overnight (1700–0800 hours) and then injected i.p. with glucose (2 g/kg of body weight). Tail blood was collected at −1, 15, 30, 60, and 120 min. Blood

PHYSIOLOGY
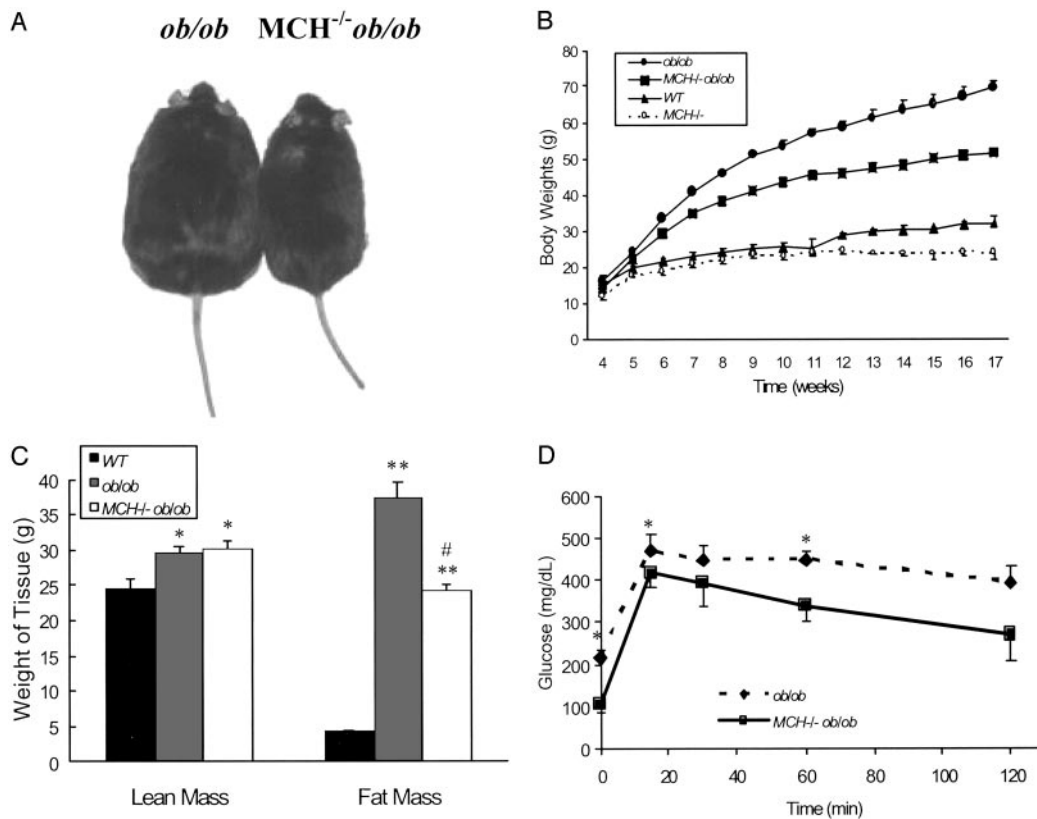
Fig. 1. Growth, body composition, and glucose tolerance. (*A*) Photograph showing body size of MCH$^{-/-}$ *ob/ob* and *ob/ob* mice at 16 weeks of age. (*B*) Weights of *ob/ob*, MCH$^{-/-}$ *ob/ob*, MCH$^{-/-}$, and WT mice over the course of 17 weeks. (*C*) Dual-energy x-ray absorptiometry analysis of 16-week-old WT (black bar), *ob/ob* (gray bar), and MCH$^{-/-}$ *ob/ob* (white bar) mice showing lean tissue mass and fat tissue mass. *, $P < 0.015$ vs. WT; **, $P < 0.0001$ vs. WT; #, $P = 0.001$ vs. *ob/ob*. (*D*) Glucose tolerance test of *ob/ob* (black diamonds) and MCH$^{-/-}$ *ob/ob* (black squares) mice at the age of 18 weeks after being fasted from 1700 hours to 0800 hours. *, $P < 0.05$ vs. MCH$^{-/-}$ *ob/ob*.

glucose levels were measured by using a glucometer (Elite, Bayer, Mishawaka, IN).

RIAs. Corticosterone was measured by using a commercially available RIA kit (ICN) according to manufacturer instructions.

Indirect Calorimetry. Metabolic rates were measured by indirect calorimetry in 12- to 14-week-old male MCH$^{-/-}$ *ob/ob*, *ob/ob*, and WT mice by using an eight-chamber open-circuit Oxymax system component of the comprehensive laboratory animal monitoring system (Columbus Instruments, Columbus, OH). Mice were maintained at ≈24°C under a 12-h light/dark cycle (light period, 0800–2000 hours). Food and water were available ad libitum. Animals were housed individually in specially built Plexiglas cages (height, 5 inches; width, 4.5 inches; depth, 8.5 inches) through which room air was passed at a flow rate of ≈0.54 liters/min. Exhaust air from each chamber was sampled at 1-h intervals for a period of 1 min; O_2 and CO_2 content of exhaust was determined by comparison to O_2 and CO_2 content of standardized sample air. Mice were acclimatized to cages for 48 h before beginning recordings, weighed, and then underwent 24 h of monitoring.

Motor Activity. Ambulatory activity was evaluated by using an OPTO-M3 sensor system (Columbus Instruments). Consecutive adjacent photobeam breaks were scored as an ambulatory count. Cumulative ambulatory activity counts were recorded every hour for 24 h.

Body Composition. Fat and lean body mass were determined by using dual-energy x-ray absorptiometry (Lunar PIXImus2 mouse

densitometer, General Electric Medical Systems, Madison, WI) as described by the manufacturer. The machine was calibrated daily by using a phantom provided by the manufacturer. The image-acquisition time was <5 min. The interassay coefficient of variation was 0.22%. Before scanning, mice were injected i.p. with a 1:1 mixture of tribromoethanol/*tert*-amyl alcohol (0.015 ml/g of body weight).

Cold Exposure. To determine thermoregulatory ability of 30-week-old WT, *ob/ob*, and MCH$^{-/-}$ *ob/ob* mice, individual mice were placed in a 2-liter beaker with 1-inch-deep bedding. The beaker was placed on ice in an insulated chamber in which air temperature was 4°C. Temperature was measured at 15-min intervals for 1 h by using a rectal probe.

Immunoblotting. Interscapular brown fat from 34-week-old mice ($n = 4$ per group) was washed twice in cold buffer containing Hepes, EDTA, and sucrose (HES buffer: 20 mM Hepes, pH 7.4/1 mM EDTA/255 mM sucrose/1 µg/ml leupeptin/10 µg/ml aprotinin/1 mM phenylmethylsulfonyl fluoride), homogenized for 1 min in an equal volume of HES by using a polytron homogenizer, and centrifuged at $3,000 \times g$ for 10 min at 4°C, and supernatants containing total cell lysates were collected. Protein concentrations were determined by Bradford analysis. Samples were solubilized in Laemmli sample buffer, and equal amounts of protein (60 µg) were separated by SDS/PAGE. Proteins were transferred to nitrocellulose and probed with an affinity-purified goat polyclonal α-UCP-1 antibody (Santa Cruz Biotechnology). Signals were visualized using an anti-goat IgG-HRP-conjugated secondary antibody (Santa Cruz Biotechnology) and an enhanced chemiluminescence detection kit

Segal-Lieberman *et al.*
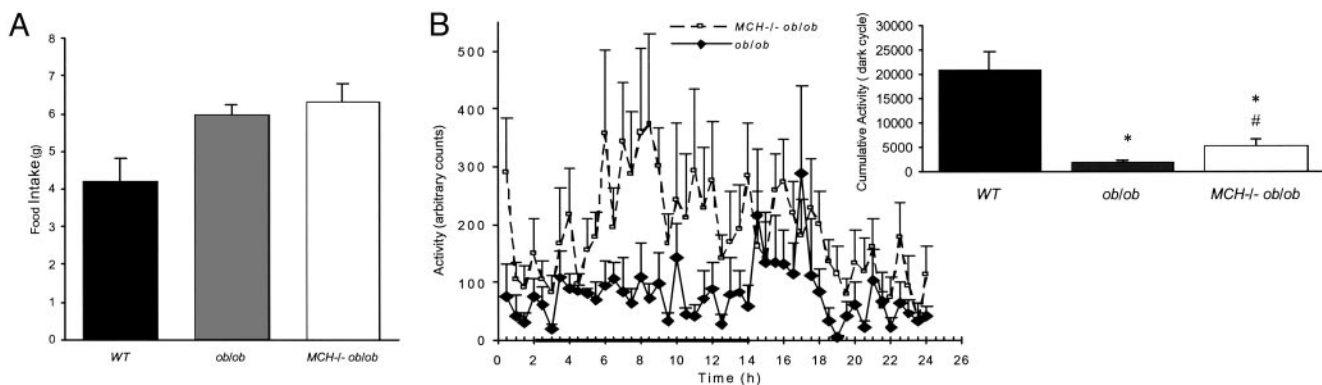
Fig. 2. Food intake and motor activity. (*A*) Food intake of 12- to 14-week-old male WT, MCH$^{-/-}$ *ob*/*ob*, and *ob*/*ob* mice measured over 24 h. (*B*) Locomotor activity of 12- to 14-week-old MCH$^{-/-}$ *ob*/*ob* (*n* = 6) and *ob*/*ob* (*n* = 6) mice during a 24-h time period while individually housed in the comprehensive laboratory animal monitoring system. (*Inset*) Cumulative dark-cycle activity for each animal group. ∗, *P* < 0.05 vs. WT; #, *P* < 0.001 vs. *ob*/*ob*.

(Perkin–Elmer Life Sciences, Boston). Signal intensities were quantified by using a densitometer (Molecular Dynamics).

Determination of Liver Stearoyl-CoA Desaturase 1 (SCD-1) mRNA Expression and Liver Triglyceride Content. Liver SCD-1 gene expression was quantified by real-time PCR with the ABI Prism 7700 sequence detection system (Applied Biosystems). Total RNA was extracted from 50- to 100-mg liver samples from WT, *ob*/*ob*, and MCH$^{-/-}$ *ob*/*ob* mice by using the Ultraspec RNA isolation system (Biotecx Laboratories, Houston) as described (8). A 1-μg sample of RNA was used to synthesize cDNA by using the Advantage one-step RT-PCR kit (CLONTECH) as described by the manufacturer. TaqMan primers and probes were designed by using Primer3 (9). The primers used were 5′-CATCATTCTCATGGTC-CTGCT-3′ (sense) and 5′-CCAGTCGTACACGTCATTTT-3′ (antisense). Primers (300 nM) were optimized to amplify cDNA but not genomic DNA and to generate a single PCR product. For amplification of SCD-1, a 5-μl cDNA sample was used in a 40-μl PCR (SYBRGreen, Applied Biosystems). Thermocycler conditions comprised an initial holding stage at 50°C for 2 min followed by 95°C for 10 min followed by a PCR program consisting of 95°C for 15 sec and 60°C for 60 sec for 40 cycles. Samples were run in duplicate. To control for input and the integrity of RNA, TATA-binding protein (primers kindly provided by Bruce Spiegleman, Dana–Farber Cancer Institute, Boston) was amplified likewise from the same cDNA in parallel PCRs. Results are expressed as arbitrary units of SCD-1 mRNA normalized by TATA-binding protein expression.

To determine liver triglyceride content, 100 mg of tissue was homogenized in 1 ml of a solution containing 150 mM sodium chloride, 0.1% Triton X-100, and 10 mM Tris, pH 8.0 as described (10) and incubated at 60°C for 1 h. Triglycerides were measured by using the GPO-Trinder triglyceride assay (Sigma Diagnostics, St. Louis). Glycerol standards (Sigma Diagnostics) were used to generate a standard curve.

Statistics. Values are reported as group means ± SE. Interactions between genotype and physiological parameters across light and dark cycles were analyzed by one-way ANOVA (factorial) when appropriate. The level of significance was taken as *P* < 0.05. Statistical comparisons were made by using STATVIEW software (Abacus Concepts, Berkeley, CA).

Results

Body Weights, Body Composition, and Glucose Tolerance. Weights of animals were monitored on a weekly basis beginning at 4 weeks of age until animals were 17 weeks old, after which they were weighed monthly up to 6 months of age. As shown in Fig. 1*A*, the phenotype

of MCH$^{-/-}$ *ob*/*ob* animals was visually distinguishable from that of *ob*/*ob* animals. By 7 weeks of age MCH$^{-/-}$ *ob*/*ob* mice weighed 11.5% less than their *ob*/*ob* counterparts (35.77 ± 1.25 vs. 40.44 ± 0.87 g, respectively; *P* = 0.0018), and by 12 weeks of age MCH$^{-/-}$ *ob*/*ob* mice weighed 21.6% less than the *ob*/*ob* controls (46.03 ± 1.00 vs. 58.71 ± 1.66 g, respectively; *P* < 0.0001) (Fig. 1*B*). At 6 months, *ob*/*ob* mice weighed 86.5 ± 2.40 g, whereas MCH$^{-/-}$ *ob*/*ob* animals weighed 61.2 ± 1.60 g (data not shown). Body composition was determined at 16 weeks of age in MCH$^{-/-}$ *ob*/*ob* mice weighing 18.7% less than their age-matched *ob*/*ob* counterparts (54.49 ± 2.26 vs. 67 ± 1.80 g, respectively). MCH$^{-/-}$ *ob*/*ob* mice had significantly less fat tissue than *ob*/*ob* mice (24.3 ± 0.75 vs. 37.53 ± 2.20 g; *P* = 0.0001), representing 44.7% and 55.8% of the total body mass of MCH$^{-/-}$ *ob*/*ob* and *ob*/*ob* mice, respectively (*P* = 0.0006). The lean body mass for MCH$^{-/-}$ *ob*/*ob* mice was 30.13 ± 1.30 g (55.3% of total weight), whereas that for *ob*/*ob* mice was 29.6 ± 0.85 g (46.4% of total weight). Data from similarly aged WT animals are included for comparison (Fig. 1*C*). Glucose tolerance was assessed in 18-week-old *ob*/*ob* and MCH$^{-/-}$ *ob*/*ob* mice weighing 64.3 and 52.0 g, respectively. As shown in Fig. 1*D*, fasting glucose was significantly lower for the MCH$^{-/-}$ *ob*/*ob* mice (106 ± 18.65 mg/dl) compared with their *ob*/*ob* counterparts (216.57 ± 17.54 mg/dl), *P* = 0.001. Over the course of a 2-h glucose tolerance test, glucose levels for MCH$^{-/-}$ *ob*/*ob* mice ranged from 11.5% to 31.6% less than those of *ob*/*ob* mice. Similar results were seen with 9-week-old animals (data not shown). Insulin levels were also determined for control, MCH$^{-/-}$, *ob*/*ob*, and MCH$^{-/-}$ *ob*/*ob* mice. Serum insulin levels in control and MCH$^{-/-}$ mice were 2.4 ± 0.3 and 3.1 ± 1.0 ng/ml, respectively (*P* = not significant). In contrast, despite improved glucose tolerance, MCH$^{-/-}$ *ob*/*ob* mice remained hyperinsulinemic (73.7 ± 18.5 ng/ml), with levels that trended slightly higher than levels for *ob*/*ob* mice (63.9 ± 7.8 ng/ml), *P* = not significant.

Food Intake and Activity. We also measured food intake and locomotor activity in 12- to 14-week-old WT, *ob*/*ob*, and MCH$^{-/-}$ *ob*/*ob* mice. In the latter two groups (Fig. 2*A*), food intake was similar; MCH$^{-/-}$ *ob*/*ob* mice ate on average 6.33 g/day, and *ob*/*ob* mice ate 5.98 g/day (*P* = not significant). This is an almost 2 g increase over food intake seen in WT mice, which averaged 4 g/day. Locomotor activity was monitored for 24 h as described in *Materials and Methods*; *ob*/*ob* animals exhibited minimal locomotor activity and no diurnal variation (Fig. 2*B*). In comparison, double-null mice showed an almost 3-fold increase in activity with a normal diurnal pattern (Fig. 2*B*). Average counts per hour were 441 ± 41 for MCH$^{-/-}$ *ob*/*ob* and 152 ± 15 for *ob*/*ob* (*P* < 0.001). Total activity counts during the dark cycle for the former and latter were 2,646 ± 102 vs. 916 ± 19, respectively (*P* < 0.001), whereas WT animals of
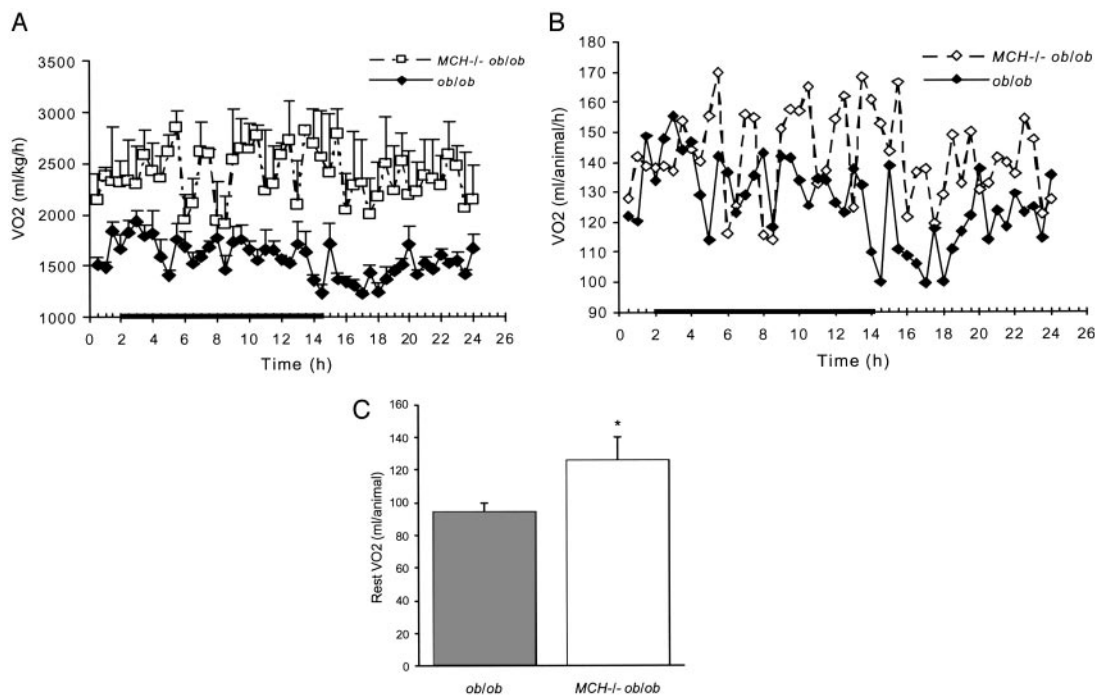
Fig. 3. VO$_2$. (*A*) VO$_2$ for 12- to 14-week-old MCH$^{-/-}$ *ob/ob* (*n* = 3) and *ob/ob* (*n* = 5) mice corrected for the weight of the animal (ml/kg per h). (*B*) Per-animal, per-hour VO$_2$, not corrected for body weight. (*C*) Resting VO$_2$ for 12- to 14-week-old MCH$^{-/-}$ *ob/ob* (*n* = 3) and *ob/ob* (*n* = 5) mice measured per animal (ml per animal per h). ∗, *P* = 0.04 vs. *ob/ob* mice.

similar age had total activity counts of >20,000 during the dark cycle (Fig. 2*B Inset*).

Metabolic Analysis. Oxygen consumption (VO$_2$) was evaluated in 12- to 14-week-old animals. In MCH$^{-/-}$ *ob/ob* mice, total VO$_2$ was increased throughout the day compared with *ob/ob* mice. This increase was seen both when VO$_2$ was calculated with a weight correction (Fig. 3*A*) and on a per-animal basis (Fig. 3*B*). Resting VO$_2$, assessed by measuring VO$_2$ during periods of inactivity (<10 beam breaks per hour), was increased >25% in MCH$^{-/-}$ *ob/ob* animals compared with *ob/ob* mice (Fig. 3*C*). Double-null animals had far fewer periods of inactivity (2.6 ± 0.66 h) than *ob/ob* mice (16.8 ± 2.6 h).

Cold Exposure. Thermoregulatory ability of 30-week-old WT, *ob/ob*, and MCH$^{-/-}$ *ob/ob* mice was assessed by exposing mice to an ambient temperature of 4°C for 1 h and measuring body temperature at 15-min intervals. The *ob/ob* mice had low basal body temperature compared with WT animals (35.5°C vs. 37.7°C) and exhibited a rapid and drastic drop of 9°C over 1 h compared with a 1.4°C decrease in the WT animals. MCH$^{-/-}$ *ob/ob* mice had normal initial core temperatures and a slower fall and smaller drop in temperature (5°C decrease) (Fig. 4*A*).

Brown Adipose Tissue (BAT) Uncoupling Protein 1 (UCP-1) Expression. Assessment of UCP-1 protein in BAT from 34-week-old animals revealed that UCP-1 levels were slightly decreased in *ob/ob* mice compared with WT animals (Fig. 4*B*). As seen in Fig. 4*B*, MCH$^{-/-}$ *ob/ob* animals showed a 3-fold increase in UCP-1 protein; this increase was similar to that seen in MCH$^{-/-}$ animals, in which increased energy expenditure has been reported (3).

Corticosterone Levels. MCH ablation led to an attenuation of the elevated glucocorticoid levels present in *ob/ob* animals. Corticosterone was 41 ng/ml in WT animals, >4-fold elevated at an

average of 187 ng/ml in *ob/ob* animals and reduced to 80 ng/ml in MCH$^{-/-}$ *ob/ob* animals (Fig. 5*A*).

Liver Triglyceride and SCD-1 mRNA Expression. Liver weight was the same in control and MCH$^{-/-}$ mice (1.5 g), whereas *ob/ob* livers averaged 5.96 g and MCH$^{-/-}$ *ob/ob* livers averaged 5.33 g. Hepatic triglyceride content (Fig. 5*B*) mirrored differences in weight as did liver histology. Histology was normal in WT and MCH$^{-/-}$ mice (data not shown), whereas livers from *ob/ob* and MCH$^{-/-}$ *ob/ob* animals showed significant hepatosteatosis (Fig. 5*C*). However, SCD-1 expression was partially corrected. Liver SCD-1 was increased in *ob/ob* animals compared with control animals. In MCH$^{-/-}$ *ob/ob* mice, SCD-1 expression was intermediate between *ob/ob* and WT animals (Fig. 5*D*).

Discussion

MCH is a key central regulator of energy balance. Initially identified as a neuropeptide up-regulated in hypothalami of *ob/ob* mice (2), MCH administered intracerebroventricularly into rats causes a rapid, robust hyperphagic response. Ablation of the prepro-MCH gene leads to a lean phenotype secondary to hypophagia and increased energy expenditure (3), and chronic infusions of MCH lead to weight gain and hyperinsulinemia (6, 7). Ablation of MCHR-1, the rodent receptor for MCH, also leads to leanness secondary to increased locomotor activity (11, 12). Thus, MCH affects both energy intake and expenditure (11, 12).

Leptin, the *ob* gene product, is an important mediator of energy balance (13–15) and modulates a number of appetite-regulating, hypothalamic neuropeptides including agouti-related peptide (AgRP) (16), neuropeptide Y (NPY) (17), proopiomelanocortin, (18) and cocaine- and amphetamine-regulated transcript (19, 20) in the arcuate nucleus and MCH in the lateral hypothalamus (21). The orexigenic (appetite-stimulating) neuropeptides NPY and AgRP, which are coexpressed within the same cell population in the arcuate nucleus, are up-regulated in the absence of leptin. This up-regulation was suggested to contribute to the *ob/ob* phenotype
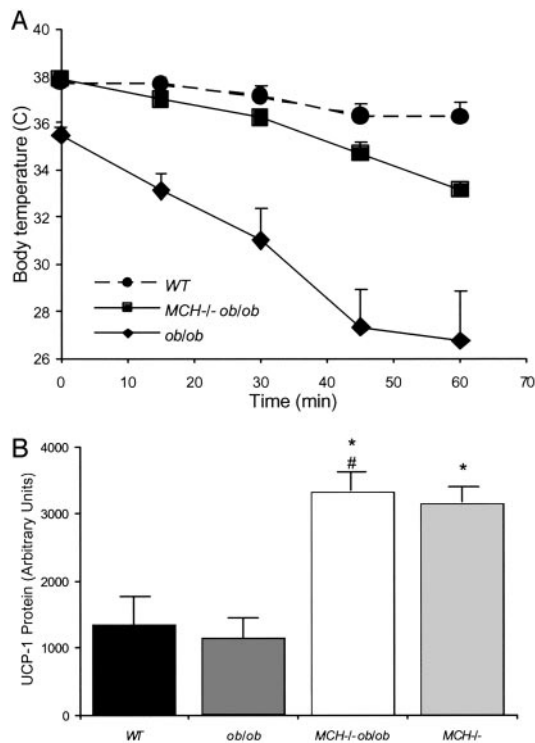
Fig. 4. Thermoregulation and expression of BAT UCP-1 expression. (*A*) Body temperature of 30-week-old WT, *ob*/*ob*, and MCH$^{-/-}$ *ob*/*ob* mice exposed to 4°C, measured every 15 min. (*B*) UCP-1 protein levels of BAT taken from 34-week-old WT, *ob*/*ob*, MCH$^{-/-}$ *ob*/*ob*, and MCH$^{-/-}$ mice (*n* = 4 per group). Results are means ± SE for three immunoblots. *, $P < 0.05$ vs. WT; #, $P = 0.002$ vs. *ob*/*ob*.

(17, 22). In support of this notion, it has been shown that NPY ablation in *ob*/*ob* mice attenuated aspects of their obese phenotype including hyperphagia, although substantial obesity remained, and the effects of NPY ablation on feeding vs. energy expenditure were not fully explored (23). The effect of AgRP ablation on the *ob*/*ob* phenotype has yet to be reported.

Another important orexigenic neuropeptide is MCH, which is expressed in the lateral hypothalamus and overexpressed in *ob*/*ob* mice. Removing MCH from leptin-deficient *ob*/*ob* mice leads to a major suppression of the phenotype; double-null mice were markedly leaner than *ob*/*ob* mice by 6 weeks of age. By 17 weeks, MCH$^{-/-}$ *ob*/*ob* animals weighed 26% less than *ob*/*ob* mice, a difference that persisted until the end of the observation period at 6 months. Decreased weight was secondary to a decrease in body fat because lean body mass was unaffected. Consistent with lower body fat, MCH$^{-/-}$ *ob*/*ob* animals had improved glucose tolerance. Despite reduced adiposity and improved glucose tolerance, double-null mice were as hyperinsulinemic as *ob*/*ob* mice; both groups had serum insulin >25-fold higher than levels in control animals. These findings suggest that the double-null mice have improved insulin sensitivity that is sufficient to improve glucose tolerance but still requires sustained hyperinsulinemia. Alternatively, glucose utilization may be improved secondary to increased demand for fuel by muscle associated with increased activity and by BAT secondary to increased basal energy expenditure. MCH ablation also led to a marked reduction in the high corticosterone levels typically seen in *ob*/*ob* mice. The mechanism of this attenuation remains unknown but may reflect changes in proopiomelanocortin or adrenocorticotropic hormone expression.

Because MCH is an orexigenic peptide, we expected that MCH ablation would suppress obesity in *ob*/*ob* mice at least in part through suppression of hyperphagia. Surprisingly, this was not the case. Amelioration of the *ob*/*ob* phenotype was entirely secondary to increased energy expenditure because double-null animals had hyperphagia equal to that of *ob*/*ob* mice. This result suggests that the state of leptin deficiency activates a battery of orexigenic mediators (including NPY, AgRP, MCH, and others), and maximal hyperphagia persists in the unique absence of MCH, which further implies that, although NPY/AgRP neurons have projections to MCH neurons in the lateral hypothalamus, the contribution of
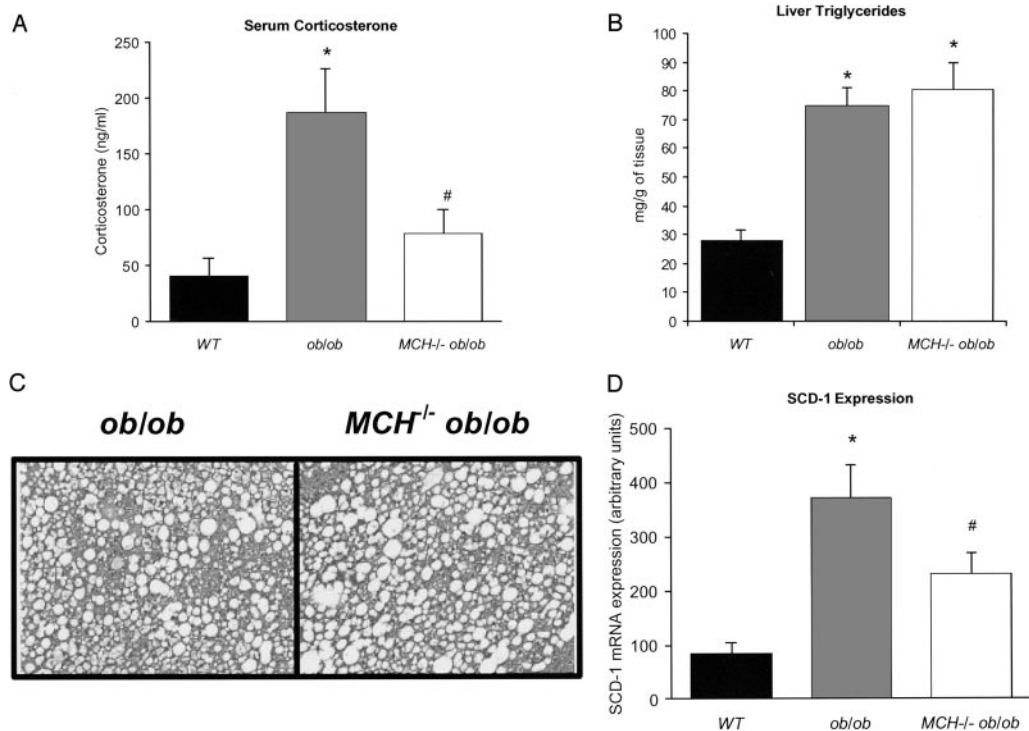
Fig. 5. Corticosterone levels, liver triglyceride, and SCD-1 mRNA expression. (*A*) Serum corticosterone in WT, *ob*/*ob*, and MCH$^{-/-}$ *ob*/*ob* mice. *, $P = 0.014$ vs. WT; #, $P = 0.02$ vs. *ob*/*ob*. (*B*) Hepatic triglyceride content of WT, *ob*/*ob*, and MCH$^{-/-}$ *ob*/*ob* mice. *, $P < 0.0005$. (*C*) Photomicrographs showing liver histology from *ob*/*ob* and MCH$^{-/-}$ *ob*/*ob* mice. (*D*) SCD-1 mRNA expression in the liver of WT, *ob*/*ob*, and MCH$^{-/-}$ *ob*/*ob* mice. *, $P < 0.007$ vs. WT; #, $P < 0.02$ vs. *ob*/*ob*.

these neurons to hyperphagia in the *ob/ob* mouse may not require MCH.

These data also indicate that MCH plays a major role in the *ob/ob* phenotype through effects on energy expenditure. Although subordinated to the observation that MCH is a potent orexigenic peptide, hints of such an action were seen in our previous study of mice with prepro-MCH ablation (3). In addition to hypophagia and leanness these mice also had increased energy expenditure. Subsequent studies in mice lacking MCHR revealed these animals to be hyperphagic but lean secondary to increased locomotor activity (11). Differences between the prepro-MCH null mouse and the MCHR-1 null mouse might be attributed to the absence of two other MCH gene transcripts, neuropeptide EI (NEI) and neuropeptide GE (NGE), neuropeptides with unknown roles, in the ligand knockout mouse. It is also possible that the loss of both NEI and NGE may contribute to the phenotypic alteration of our MCH$^{-/-}$ *ob/ob* mice. Future studies may focus on resolving this issue. One approach in defining the roles of NEI and NGE in attenuating the *ob/ob* mouse phenotype would be to generate a MCHR-1-deficient *ob/ob* mouse model, which would represent a model of MCH deficiency in which NEI and NGE are preserved.

The present studies reveal a powerful influence of MCH on regulation of body temperature and thermogenesis. Both basal thermoregulation and shivering thermogenesis were improved in MCH$^{-/-}$ *ob/ob* mice, and these animals also showed an elevation in UCP-1 expression in BAT. Interestingly, a very recent report indicates that MCH infusions can suppress UCP-1 and decrease body temperature (6). These findings suggest a role for MCH in regulating the activity of the sympathetic nervous system (SNS) as relates to energy expenditure pathways. MCH, downstream of leptin, seems to be required for the full suppression of SNS activity seen in the *ob/ob* mouse. In the absence of MCH, the SNS remains somewhat activated even in a leptin-deficient state, ameliorating obesity via effects on energy expenditure. It is also possible that MCH is required for full leptin action because it modifies other downstream mediators of leptin action such as NPY or α-MSH. Further studies will be required to assess the impact of loss of MCH on the activity of the SNS as well as on the expression of other neuropeptides important in regulating energy balance and to characterize the detailed neural circuitry related to this effect.

Leptin deficiency is known to induce expression of the gene encoding the lipid-modifying enzyme SCD-1 (24, 25), and ablation of this gene markedly suppresses obesity and fatty liver in *ob/ob* mice, without suppressing hyperphagia, through effects to increase energy expenditure. We evaluated potential changes in SCD-1 expression in double-null mice. We confirmed the marked induction of SCD-1 mRNA in *ob/ob* liver compared with WT mice and observed that hepatic SCD-1 expression was decreased by 50% in the double-null mice compared with *ob/ob* animals. Insulin increases SCD-1 activity (26, 27); however, despite their reduced adiposity, MCH$^{-/-}$ *ob/ob* mice were as hyperinsulinemic as *ob/ob* mice. Thus, the decrease in SCD-1 expression in MCH$^{-/-}$ *ob/ob* mice was not due to decreased insulin, which suggests that MCH may be involved in pathways regulating SCD-1 expression. Despite a marked reduction in total body fat in double-null animals, both liver weight and liver fat were comparable to the livers of *ob/ob* mice. An explanation for the observed reduction in SCD-1 expression without a decrease in liver fat in MCH$^{-/-}$ *ob/ob* mice may be that the partial correction of SCD-1 is insufficient to lead to a change in hepatic fat content.

In summary, MCH ablation in *ob/ob* mice leads to a dramatic attenuation of obesity, despite unabated hyperphagia, secondary to increased metabolic rate and increased locomotor activity. These findings suggest a previously unknown role for MCH as a critical link among metabolism, locomotion, and thermoregulation and underscore a critical integrative role for MCH in the regulation of energy homeostasis.

1. Bittencourt, J. C., Presse, F., Arias, C., Peto, C., Vaughan, J., Nahon, J. L., Vale, W. & Sawchenko, P. E. (1992) *J. Comp. Neurol.* **319,** 218–245.
2. Qu, D., Ludwig, D. S., Gammeltoft, S., Piper, M., Pelleymounter, M. A., Cullen, M. J., Mathes, W. F., Przypek, R., Kanarek, R. & Maratos-Flier, E. (1996) *Nature* **380,** 243–247.
3. Shimada, M., Tritos, N. A., Lowell, B. B., Flier, J. S. & Maratos-Flier, E. (1998) *Nature* **396,** 670–674.
4. Rossi, M., Choi, S. J., O'Shea, D., Miyoshi, T., Ghatei, M. A. & Bloom, S. R. (1997) *Endocrinology* **138,** 351–355.O. S.
5. Ludwig, D. S., Tritos, N. A., Mastaitis, J. W., Kulkarni, R., Kokkotou, E., Elmquist, J., Lowell, B., Flier, J. S. & Maratos-Flier, E. (2001) *J. Clin. Invest.* **107,** 379–386.
6. Ito, M., Gomori, A., Ishihara, A., Oda, Z., Mashiko, S., Matsushita, H., Yumoto, M., Sano, H., Tokita, S., Moriya, M., *et al.* (2003) *Am. J. Physiol.* **284,** E940–E945.
7. Della-Zuana, O., Presse, F., Ortola, C., Duhault, J., Nahon, J. L. & Levens, N. (2002) *Int. J. Obes. Relat. Metab. Disord.* **26,** 1289–1295.
8. Bradley, R. L., Kokkotou, E. G., Maratos-Flier, E. & Cheatham, B. (2000) *Diabetes* **49,** 1073–1077.
9. Rozen, S. & Skaletsky, H. J. (2000) in *Bioinformatics Methods and Protocols: Methods in Molecular Biology,* eds. Krawetz, S. & Misener, S. (Humana, Totowa, NJ), pp. 365–386.
10. Okunu, A., Tamemoto, H., Tobe, K., Ueki, K., Akanuma, Y., Fujiwara, T., Horikoshi, H. & Yazaki, Y. (1998) *J. Clin. Invest.* **101,** 1354–1361.
11. Marsh, D. J., Weingarth, D. T., Novi, D. E., Chen, H. Y., Trumbauer, M. E., Chen, A. S., Guan, X. M., Jiang, M. M., Feng, Y., Camacho, R. E., *et al.* (2002) *Proc. Natl. Acad. Sci. USA.* **99,** 3240–3245.
12. Chen, Y., Hu, C., Hsu, C. K., Zhang, Q., Bi, C., Asnicar, M., Hsiung, H. M., Fox, N., Slieker, L. J., Yang, D. D., Heiman, M. L. & Shi, Y. (2002) *Endocrinology* **143,** 2469–2477.
13. Friedman, J. M. & Halaas, J. L. (1998) *Nature* **395,** 763–770.
14. Spiegelman, B. M. & Flier, J. S. (2001) *Cell* **104,** 531–543.
15. Zhang, Y., Proenca, R., Maffei, M., Barone, M., Leopold, L. & Friedman, J. M. (1994) *Nature* **372,** 425–432.
16. Broberger, C., Johansen, J., Johansson, C., Schalling, M. & Hokfelt, T. (1998) *Proc. Natl. Acad. Sci. USA* **95,** 15043–15048.
17. Schwartz, M. W., Seeley, R. J., Campfield, L. A., Burn, P. & Baskin, D. G. (1996) *J. Clin. Invest.* **98,** 1101–1106.
18. Mizuno, T. M. & Mobbs, C. V. (1999) *Endocrinology* **140,** 814–817.
19. Ahima, R. S., Kelly, J., Elmquist, J. K. & Flier, J. S. (1999) *Endocrinology* **140,** 4923–4931.
20. Elias, C. F., Lee, C., Kelly, J., Aschkenasi, C., Ahima, R. S., Couceyro, P. R., Kuhar, M. J., Saper, C. B. & Elmquist, J. K. (1998) *Neuron* **21,** 1375–1385.
21. Tritos, N. A., Mastaitis, J. W., Kokkotou, E. & Maratos-Flier, E. (2001) *Brain Res.* **895,** 160–166.
22. Stephens, T. W., Basinski, M., Bristow, P. K., Bue-Valleskey, J. M., Burgett, S. G., Craft, L., Hale, J., Hoffmann, J., Hsiung, H. M., Kriauciunas, A., *et al.* (1995) *Nature* **377,** 530–532.
23. Erickson, J. C., Hollopeter, G. & Palmiter, R. D. (1996) *Science* **274,** 1704–1707.
24. Ntambi, J. M., Miyazaki, M., Stoehr, J. P., Lan, H., Kendziorski, C. M., Yandell, B. S., Song, Y., Cohen, P., Friedman, J. M. & Attie, A. D. (2002) *Proc. Natl. Acad. Sci. USA* **99,** 11482–11486.
25. Cohen, P., Miyazaki, M., Socci, N. D., Hagge-Greenberg, A., Liedtke, W., Soukas, A. A., Sharma, R., Hudgins, L. C., Ntambi, J. M. & Friedman, J. M. (2002) *Science* **297,** 240–243.
26. Waters, K. M. & Ntambi, J. M. (1994) *J. Biol. Chem.* **269,** 27773–27777.
27. Lefevre, P., Diot, C., Legrand, P. & Douaire, M. (1999) *Arch. Biochem. Biophys.* **368,** 329–337.